acids 744 to 2460 [M. E. Ewen, Y. Xing, J. B. Lawrence, D. M. Livingston, *Cell* **66**, 1155 (1991)]. For EMSAs [A. Barberis, G. Superti-Furga, M. Busslinger, *ibid.* **50**, 347 (1987)], the purified recombinant proteins (~100 ng) were incubated with 0.5 pmol of ^{32}P-labeled probe for 30 min at 22°C in 15 μl of a buffer containing 50 mM tris-HCl (pH 8.0), 50 mM NaCl, 10% (v/v) glycerol, 0.2 mM EDTA, 1 mM dithiothreitol, and polydeoxyadenylic-deoxythymidylic acid (poly[dA/dT]) (67 ng/μl). Probes were labeled by filling in 5′ overhanging ends of four to seven bases. Samples were run on 4% nondenaturing polyacrylamide gels in 0.5× tris-borate EDTA (TBE) at 4°C and 10 V/cm. Gels were exposed to x-ray films and quantitatively evaluated with a Molecular Dynamics PhosporImager. The following double-stranded probes were used: B-*myb* (*3*), 5′-GGCGCCGACGCACTTGGCGGGAGATAGGAAAGTGGTTCTGTG (E2F site underlined); mutated B-*myb* site, 5′-GGCGCCGACGCACTTGGCTGGAGATAGGAAAGTGGTTCTGTG; E2 promoter, 5′-gatcGACTAGTTTCGCGCCCTTTCTActag (lowercase letters represent unrelated sequences used for the fill-in labeling reactions); unrelated probe, 5′-GATCCTCTCACCTGCTGCTAG [NIP-5′; K. Engeland, N. C. Andrews, B. Mathey-Prevot, *J. Biol. Chem.* **270**, 24572 (1995)].

6. For in vitro DMS footprinting, a B-*myb* coding strand oligonucleotide was end-labeled, purified, and annealed to the noncoding strand. Binding reactions were carried out as described (*5*). Two microliters of 2% DMS were added, and the methylation reaction was stopped after 3 min by adding 2 μl of 60 mM β-mercaptoethanol. The samples were run on a 4% gel and transferred to ion-exchange paper. Both the shifted and unshifted (free probe) bands were cut out, rinsed with tris-EDTA (TE) buffer, and eluted with TE buffer containing 1.5 M NaCl at 65°C. The eluted DNA was extracted with chloroform, precipitated, and dissolved in water. Equal radioactive amounts of free probe and shifted complex were cleaved with 10% piperidine at 95°C for 30 min. The DNA was precipitated and loaded on a 15% denaturing acrylamide gel.
7. K. Helin *et al.*, *Cell* **70**, 337 (1992); W. G. Kaelin *et al.*, *ibid.*, p. 351.
8. R. L. Beijersbergen *et al.*, *Genes Dev.* **8**, 2680 (1994); D. Ginsberg *et al.*, *ibid.*, p. 2665.
9. M. Mudryj, S. W. Hiebert, J. R. Nevins, *EMBO J.* **9**, 2179 (1990).
10. EMSA gels were evaluated with a PhosphorImager to calculate the fraction of bound probe. The following fractions were obtained: E2 promoter E2F site, 1.0% (E2F1–DP-1) and 0.8% (E2F-4–DP-1), respectively; B-*myb*, 0.7% (E2F1–DP-1) and 2.0% (E2F-4–DP-1), respectively; mutated B-*myb*, <0.01%; unrelated probe, <0.002%.
11. K. Engeland and N. Liu, unpublished data.
12. On-rates and off-rates were determined essentially as described [R. Janknecht, R. A. Hipskind, T. Houthaeve, A. Nordheim, H. G. Stunnenberg, *EMBO J.* **11**, 1045 (1992)]. The data were quantitated with a PhosphorImager. For on-rates, recombinant protein complexes were incubated at 4°C with the B-*myb* probe (*5*) and, after different incubation times, loaded on a 4% gel run at 4°C. The latest time point was used for normalization of the results (100% value). For off-rates, recombinant protein complexes and radioactive DNA probe were incubated at 22°C for 20 min to achieve maximum binding. The samples were cooled to 4°C, and a 50-fold excess of nonradioactive competitor was added. After different incubation times, samples were analyzed by EMSA. A sample without competitor served as the reference for normalization (100% value).
13. N. Liu, unpublished data.
14. F. C. Lucibello *et al.*, *EMBO J.* **14**, 132 (1995).
15. G. P. Pfeifer, S. D. Steigerwald, P. R. Mueller, B. Wold, A. D. Riggs, *Science* **246**, 810 (1989).
16. Genomic DMS footprinting was performed as described (*14, 15, 17*). The following primers were used: primer 1, 5′-TCAGGACTCAGGCTGCT; primer 2, 5′-CGAGCCGCTCCGGGCCCCAGG; and primer 3, 5′-GGCCCCAGGCGGTGCTCTCAGGCG.
17. J. Zwicker *et al.*, *EMBO J.* **14**, 4514 (1995); J. Zwicker *et al.*, *Nucleic Acids Res.* **23**, 3822 (1995).
18. J. Zwicker, unpublished data. The c-*myc* E2F site is described in F. Oswald, H. Lovec, T. Möröy, M. Lipp, *Oncogene* **9**, 2029 (1994) and in the reviews in (*1*).
19. The formation of G_0-G_1 phase– and S phase–specific E2F complexes binding to the B-*myb* probe was confirmed in our own experiments with the use of extracts from NIH 3T3 cells (N. Liu, unpublished data).
20. W. Krek *et al.*, *Cell* **78**, 161 (1994); B. D. Dynlacht, O. Flores, J. A. Lees, E. Harlow, *Genes Dev.* **8**, 1772 (1994).
21. S. J. Weintraub *et al.*, *Nature* **375**, 812 (1995).
22. Isolation of RNA and reverse transcription polymerase chain reaction (RT-PCR) were performed exactly as described (*14, 17*). A region of B-*myb* complementary DNA (cDNA) from positions +1630 to +2228 was amplified with the use of the primers 5′-GACACCCCTGCACCAGAAGTATC and 5′-GGCTGGACTTCAGGCGGCT.
23. We thank W. Kaelin, R. Bernards, N. La Thangue, R. Weinberg, and D. Livingston for E2F, DP, pRb, and p107 cDNAs. Supported by grants from DFG and BMBF. J.Z. was the recipient of a fellowship from the Boehringer-Ingelheim Fonds.

20 September 1995; accepted 16 January 1996

Rapid Degradation of the G_1 Cyclin Cln2 Induced by CDK-Dependent Phosphorylation

Stefan Lanker, M. Henar Valdivieso, Curt Wittenberg*

Cyclins regulate the major cell cycle transitions in eukaryotes through association with cyclin-dependent protein kinases (CDKs). In yeast, G_1 cyclins are essential, rate-limiting activators of cell cycle initiation. G_1-specific accumulation of one G_1 cyclin, Cln2, results from periodic gene expression coupled with rapid protein turnover. Site-directed mutagenesis of *CLN2* revealed that its phosphorylation provides a signal that promotes rapid degradation. Cln2 phosphorylation is dependent on the Cdc28 protein kinase, the CDK that it activates. These findings suggest that Cln2 is rendered self-limiting by virtue of its ability to activate its cognate CDK subunit.

The term "cyclin" was originally coined to describe dramatic fluctuations in abundance displayed by the positive regulatory subunits of CDKs during the cell division cycle (*1*). Despite the fact that most cyclins accumulate periodically, the mechanisms governing their accumulation appear to differ. The budding yeast G_1 cyclins, encoded by the *CLN1* and *CLN2* genes, accumulate during the G_1 phase and become maximal during the late G_1 phase as cells transit the start (the point at which cells commit to completion of a new cell cycle). Because the Cln proteins appear to be constitutively unstable (*2–5*), their pattern of accumulation largely reflects their pattern of gene expression. G_1 cyclin abundance is important in determining the timing of cell cycle initiation. Consequently, Cln protein instability is critical for proper regulation of cell cycle progression.

The PEST sequence (Pro, Glu, Ser, and Thr), found in all three yeast G_1 cyclins, was originally identified as a potential determinant of protein instability on the basis of the frequency of its occurrence in constitutively unstable proteins (*6*). However, it has yet to be functionally defined. Deletion of the COOH-terminal sequences of Cln2 and Cln3 that include the PEST motif results in phenotypes consistent with hyperactivation of G_1 cyclins (*7*). Furthermore, these truncations, as well as more precise deletions of PEST sequences, partially stabilize the mutant proteins (*4, 5, 8*). However, it is not clear whether the PEST sequences per se or other aspects of the PEST-containing region constitute the relevant determinants. Our analysis of the posttranslational modification of Cln2 has demonstrated the importance of Cln2 phosphorylation as a signal for its rapid turnover. Because Cln2 phosphorylation is dependent on the activity of its cognate CDK subunit, we propose that phosphorylation of Cln2 by Cdc28 couples activation of the Cln2-Cdc28 protein kinase to degradation of the Cln2 polypeptide and, thereby, renders Cln2-activated CDK activity self-limiting.

Phosphorylation of Cln2 causes its heterogeneous electrophoretic mobility as observed by SDS–polyacrylamide gel electrophoresis (SDS-PAGE) (Fig. 1A). The Cln2 species with highest mobility comigrates with bacterially expressed Cln2 polypeptide (*2*). Treatment of ^{35}S-labeled Cln2 immunoprecipitates with calf intestine alkaline phosphatase in the absence, but not in the presence, of phosphatase inhibitors resulted in the loss of the species with lower mobility. In addition, Cln2 became isotopically labeled when cells were grown in the presence of [^{32}P]orthophosphate (Fig. 1B). The phosphorylated amino acid residues were primarily phosphoserine and, to a lesser extent, phosphothreonine (Fig. 1C) .

To identify the protein kinase responsi-

S. Lanker and C. Wittenberg, Departments of Molecular Biology and Cell Biology, Scripps Research Institute, La Jolla, CA 92037, USA.
M. H. Valdivieso, Edificio Departamental, Microbiologia, Biologia, Avenida Del Campo Charro s/n, 37007 Salamanca, Spain.

*To whom correspondence should be addressed.

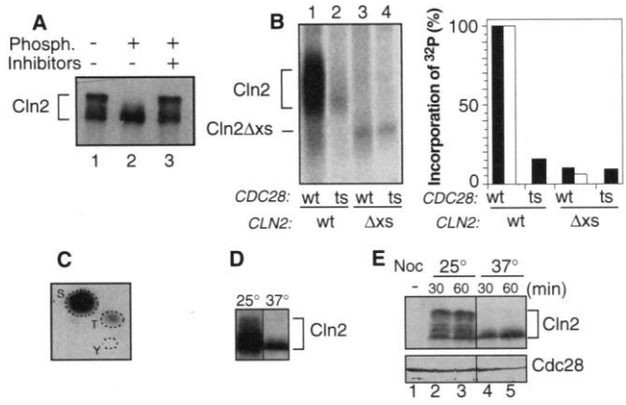

Fig. 1. Dependence of phosphorylation of Cln2 on Cdc28 protein kinase. (**A**) Extracts of cells grown in the presence of [^{35}S]methionine were immunoprecipitated with antiserum to Cln2 (*23*). Cln2 immunoprecipitates untreated (lane 1) or incubated with calf intestinal alkaline phosphatase (Phosph.) (lane 2) or with phosphatase and phosphatase inhibitors (*21*) (lane 3) were resolved by SDS-PAGE and visualized by autoradiography. (**B**) Wild-type cells (lanes 1 and 3) or temperature-sensitive (ts) *cdc28-13* mutant cells (lanes 2 and 4) expressing either wild-type *CLN2* (lanes 1 and 2) or the nonfunctional allele *cln2Δxs* (*9*) (deletion of the *CLN2* cyclin box) (lanes 3 and 4) tagged with the HA epitope (*22*) were grown in the presence of inorganic [^{32}P]orthophosphate (*24*). Extracts were incubated with monoclonal HA antibody (12CA5) (*25*) and with immunoprecipitates resolved as described (A). Quantitation of ^{32}P incorporation was performed with a PhosphorImager (closed bars, right) and is presented as a percent of that in the wild type. Quantitative results of Cln2 and Cln2Δxs phosphorylated in an in vitro immune complex protein kinase assay (*26*) are also presented (open bars, right). (**C**) Two-dimensional phosphoamino acid analysis of Cln2 phosphorylated in vivo was done as described (*27*). S, phosphoserine; T, phosphothreonine; Y, phosphotyrosine. (**D**) Cells carrying the temperature-sensitive *cdc28-13* allele and a single copy of *GAL1::CLN2* integrated at the *LEU2* locus were incubated either at the permissive (25°C) or restrictive (37°C) temperature for 120 min. Then, expression of *CLN2* was induced by addition of galactose and cells incubated for an additional 60 min at the same temperature. Extracts were analyzed by immunoblotting with antiserum to Cln2 (*2*). (**E**) The same strain was arrested by incubation in medium containing nocodazole (Noc; 15 μg/ml) for 180 min followed by a subsequent 60-min incubation at either the permissive or restrictive temperature. *GAL1::CLN2* expression was induced by addition of galactose, and extracts were analyzed by immunoblotting with antiserum to Cln2 or Cdc28 (*28*).

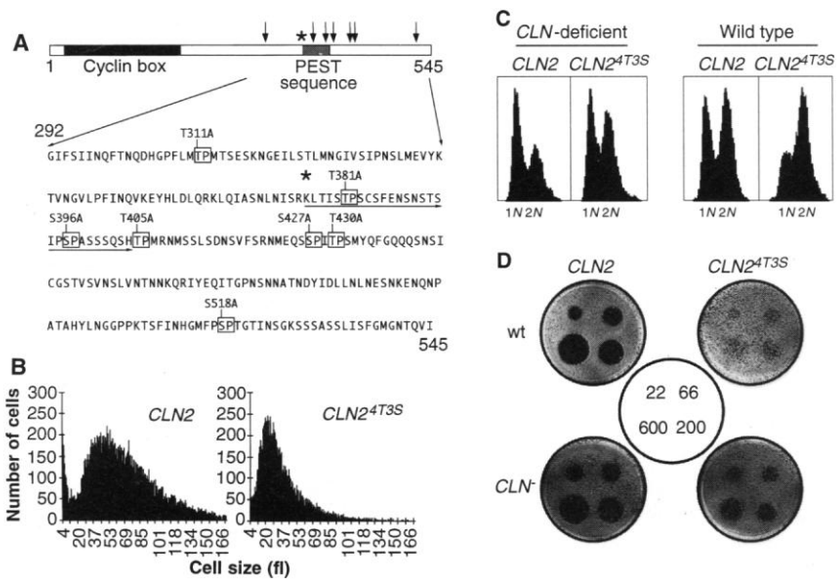

Fig. 2. Deregulated cell cycle initiation of an SP-TP–deficient *CLN2* mutant (*CLN2^{4T3S}*). (**A**) Organization of the *CLN2* protein coding region (open bar, top panel). The *CLN2* cyclin box (black bar), PEST domain (gray bar) (*6*), site of *CLN2* truncation mutants (asterisk), and the positions of SP-TP sequences (arrows; minimal Cdc28 kinase consensus sequence) are indicated. Shown below is the *CLN2* COOH-terminal amino acid sequence containing the PEST domain (underlined), the seven SP-TP sequences (boxed), and the position of the mutations described in this study (*11*). All seven S/T to A mutations (*29*) are present in the *CLN2^{4T3S}* mutant. (**B**) Cell size distributions (*30*) of asynchronous populations of *CLN*-deficient (*cln1Δcln2Δcln3ΔGAL1::CLN3*) strains carrying a single copy of either *CLN2* or *CLN2^{4T3S}* and grown in glucose so that cells are dependent on *CLN2* or *CLN2^{4T3S}*. (**C**) Flow cytometry analysis for DNA content of asynchronous populations of *CLN*-deficient or wild-type strains carrying a single copy of either *CLN2* or *CLN2^{4T3S}*. (**D**) The same strains as depicted in (C) were assayed for their capacity to respond to mating pheromone. Strains were grown for 3 days at room temperature on plates to which alpha factor was spotted in the amounts (ng) shown at the position indicated in the center panel (*31*); wt, wild-type strain; *cln-*, *CLN*-deficient strain.

ble for phosphorylation of Cln2, we evaluated Cln2's modification in cells deficient in Cdc28 protein kinase activity. *CLN2* was expressed from the inducible *GAL1* promoter in cells carrying a temperature-sensitive *cdc28-13* mutation and extracts analyzed by immunoblotting (Fig. 1D). Cln2 protein accumulating at the restrictive temperature (37°C) failed to become modified, as shown by the lack of species of lower mobility. Little in vivo incorporation of [^{32}P]phosphate into Cln2 protein was observed in *cdc28-13* mutant cells grown at the restrictive temperature (Fig. 1B). This lack of Cln2 phosphorylation appears not to result from cell cycle arrest during G_1 because modification of Cln2 expressed outside of G_1 was also dependent on functional Cdc28 (Fig. 1E). Thus, phosphorylation of Cln2 in vivo is dependent on a functional Cdc28 protein kinase.

Modification of Cln2 is also associated with the binding of Cln2 to Cdc28. Thus, a defective Cln2 mutant, Cln2Δxs (9), which is unable to bind to the Cdc28 polypeptide by virtue of a small deletion within the "cyclin box" (see below), neither displayed the characteristic heterogeneity in electrophoretic mobility nor became labeled with [^{32}P]orthophosphate in vivo or in vitro (Fig. 1B). A deficiency in Cln2 phosphorylation is observed in *cdc37* mutants where Cln2 fails to bind to Cdc28 (*10*). The modification of Cln2Δxs that was observed is unaffected by inactivation of Cdc28 and, therefore, appears not to be mediated by the Cdc28 protein kinase (Fig. 1B). The extent of phosphorylation of wild-type Cln2 is comparable to that of Cln2Δxs in a *cdc28* temperature-sensitive mutant.

Cln2 contains seven sites conforming to the minimal CDK consensus, SP or TP (Fig. 2A) (*11*). Only one of those, at position 405 (TPMR), conforms to a full CDK consensus site (S or TPXK or R, where X is any amino acid). The relative abundance of SP and TP sites is consistent both with the number of lower mobility species of Cln2 and with the extent of mobility shift associated with phosphorylation (Fig. 1). All seven putative serine or threonine phosphoacceptor sites (Fig. 2A) were mutated to alanine. This mutant gene (referred to as *CLN2^{4T3S}*) was able to complement the cell cycle defect of a strain deficient in all three *CLN* genes when introduced in a single copy under control of the wild-type *CLN2* promoter. Thus, Cln2^{4T3S} could perform its essential in vivo function.

However, the mutated gene conferred a number of phenotypes consistent with hyperactivation or hyperaccumulation of Cln2. These included (i) a decrease in the cell size distribution of an asynchronous population (Fig. 2B) as well as a decrease in the minimum size required for budding (*12*), (ii) a

decrease in the proportion of G_1 cells in an asynchronous population as judged by a decrease in both unbudded cells (*12*) or cells with a 1*N* DNA content (Fig. 2C), (iii) failure to undergo a stable G_1 phase cell cycle arrest in response to mating pheromone (Fig. 2D), and (iv) a failure to arrest homogeneously in G_1 in response to nitrogen starvation (*12*). Furthermore, the mutant gene is dominant because the same phenotypes were observed when the *CLN2*^{4T3S} gene was introduced (in a single copy) into otherwise wild-type cells (Fig. 2, C and D). This behavior is consistent with that of dominant mutants of *CLN2* in which the COOH-terminal portion of the *CLN2* open reading frame, which includes the PEST sequences, is eliminated (*9*, *12*).

To establish the source of these defects in cell cycle regulation, we biochemically analyzed strains expressing the Cln2^{4T3S} polypeptide. Mutant polypeptides that were either tagged at their COOH-terminus with the hemagglutinin (HA) epitope or untagged accumulated larger steady-state amounts than did the comparably expressed wild-type protein (Fig. 3A) (*12*), which suggests that they were stabilized. The appearance of species of Cln2 with lower mobility was completely eliminated by the mutations (Fig. 3A). The extent of incorporation of in vivo [^{32}P]orthophosphate into the mutant protein was also greatly reduced relative to that in the wild-type Cln2 protein (Fig. 3B). Thus, we assume that the mutations in Cln2^{4T3S} eliminate sites of in vivo phosphorylation.

Consistent with the increase in its steady-state amount, the Cln2^{4T3S} polypeptide was stabilized relative to wild-type Cln2. Hemagglutinin-tagged mutant or wild-type genes were placed under control of the galactose-inducible *GAL1* promoter on a centromeric plasmid. Expression of *CLN2* was transiently induced in the wild-type yeast strains and Cln2 protein abundance monitored by quantitative immunoblotting for 120 min after repression of the *GAL1* promoter. The half-life of the Cln2^{4T3S} polypeptide is 60 ± 5 min, whereas that of the wild-type Cln2 protein is 8 ± 2.5 min (Fig. 4A). This difference is apparently not an effect of expression from the *GAL1* promoter because similar values were obtained by ^{35}S labeling of wild-type Cln2 and Cln2^{4T3S} expressed from a single-copy gene under control of the wild-type *CLN2* promoter (*12*). Furthermore, the loss of modified species and the stabilization of the Cln2^{4T3S} protein did not result from the failure of Cln2^{4T3S} protein to bind and activate Cdc28. Consistent with its capacity to complement a mutant deficient in *CLN* function, the Cln2^{4T3S} protein bound to Cdc28 and activated its protein kinase activity (Fig. 3C). In contrast, the Cln2Δxs polypeptide neither bound nor activated Cdc28. We conclude that the lack of Cln2 protein modification and Cln2's stabilization are the result of the elimination of in vivo sites for phosphorylation by Cdc28.

The extent to which Cln2^{4T3S} is stabilized appears inconsistent with the stabilization associated with inactivation of Cdc28 by temperature-sensitive mutations (*4*, *12*, *13*). Furthermore, the Cln2Δxs protein is only about twofold more stable than wild-type Cln2 despite its inability to bind Cdc28 and to become phosphorylated. Both of these results could be explained if Cln2 that fails to bind Cdc28 is degraded by a mechanism that is independent of phosphoryl-

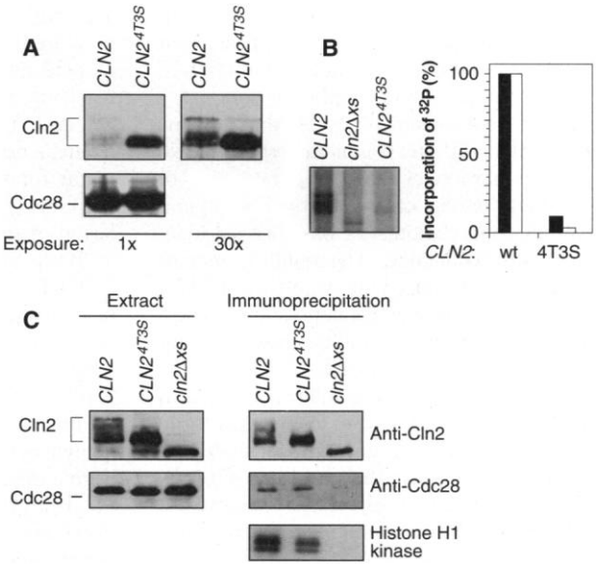

Fig. 3. Increased accumulation and decreased phosphorylation of Cln2^{4T3S}. (**A**) Steady-state amount of Cln2. Extracts of *CLN*-deficient cells containing a single copy of either *CLN2* or *CLN2*^{4T3S} under control of the *CLN2* promoter were separated by SDS-PAGE and blotted to polyvinylidene fluoride membranes. Membranes were probed with antiserum to Cln2 (upper panel) or Cdc28 (lower panel), and the relative time of exposure is indicated. (**B**) Cln2 phosphorylation. Extracts of strains expressing *CLN2* (lane 1), *cln2Δxs* (lane 2), or *CLN2*^{4T3S} (lane 3) from the *GAL1* promoter, each tagged with the HA epitope, were immunoprecipitated with monoclonal antibodies to HA. The resulting Cln2-Cdc28 immune complexes were incubated with [γ-^{32}P]ATP (*26*) for 30 min at 30°C, separated by SDS-PAGE, and visualized by autoradiography (left). Quantitation of ^{32}P incorporation was done with a PhosphorImager (right) and is presented as a percent of that in the wild type. In vivo incorporation of ^{32}P into Cln2 and Cln2^{4T3S} is also presented. Bars are as in Fig. 1B. (**C**) Binding and activation of Cdc28 kinase by Cln2^{4T3S}. Proteins from extracts of strains expressing wild-type *CLN2*, *CLN2*^{4T3S}, or *cln2Δxs*, each carrying the HA epitope, were immunoblotted with monoclonal antibodies to HA or antiserum to Cdc28 (left) or were immunoprecipitated with monoclonal antibodies to HA (right). The resulting immunoprecipitates were either immunoblotted with antiserum to Cln2 or Cdc28 (upper two right panels) or assayed for histone H1 kinase activity (*26*) with [γ-^{32}P]ATP and then analyzed by SDS-PAGE and autoradiography (lower right panel).

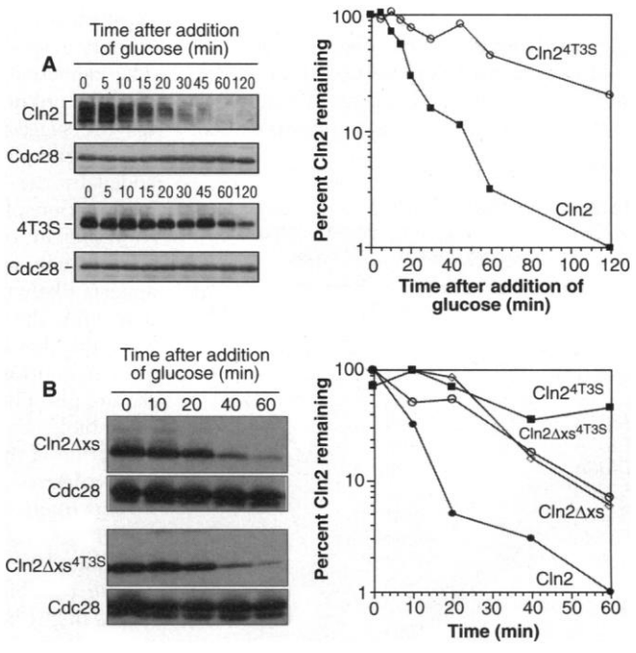

Fig. 4. Stability of Cln2 mutant proteins. (**A**) Increased stability of Cln2^{4T3S}. Wild-type *CLN2* or the *CLN2*^{4T3S} allele, both under control of the *GAL1* promoter and containing the HA epitope tag, were expressed for 40 min and then repressed by addition of glucose. Extracts prepared from samples taken at the indicated times were analyzed by SDS-PAGE and immunoblotting with monoclonal antibodies to HA or antiserum to Cdc28. Abundance of Cln2 protein was determined by densitometric analysis of the Cln2 band compared with serial dilutions of a Cln2 standard (right). (**B**) Decreased stability of a version of Cln2^{4T3S} (Cln2Δxs^{4T3S}) (*32*) having a deletion of its cyclin box. Protein stability of Cln2, Cln2^{4T3S}, Cln2Δxs, or Cln2Δxs^{4T3S} was analyzed as described above (right).

ation because Cln2 binds Cdc28 less effectively in a temperature-sensitive *cdc28* mutant at the restrictive temperature (*12*). To test this hypothesis, we constructed a version of $Cln2^{4T3S}$ ($Cln2\Delta xs^{4T3S}$) having the same deletion within the cyclin box as Cln2Δxs and evaluated its stability (Fig. 4B). As predicted, this mutant protein was degraded with kinetics similar to those of Cln2Δxs, having a half-life of only ~18 min (relative to 60 min for $Cln2^{4T3S}$ and 8 min for wild-type Cln2). Thus, it appears that degradation of Cln2 that fails to bind Cdc28 does not depend on phosphorylation.

Because it remained possible that any one of the SP or TP sites was alone responsible for the stabilization of $Cln2^{4T3S}$, the serine or threonine residue of each of the seven putative phosphorylation sites was changed independently to alanine. The resulting mutant genes were introduced into wild-type or *CLN*-deficient cells in a single copy under control of the *CLN2* promoter and evaluated both for function and stability (Table 1). Each of the mutant *CLN2* genes was fully functional, as judged by their ability to complement the inviability of a strain deficient in functional *CLN* genes (*cln1Δcln2Δcln3ΔGAL1::CLN3*). When compared to cells transformed with a wild-type *CLN2* gene, none of the cells rescued by single-site mutants had an altered phenotype.

To evaluate the effect of these mutations on protein stability, we analyzed the accumulation of Cln2 protein by immunoblotting extracts from asynchronous cultures of strains carrying the individual mutant *CLN2* alleles as the only *CLN2* gene. Only the S396A and S427A mutations (*11*) resulted in detectable hyperaccumulation of Cln2 protein (Table 1) (*12*). To analyze the half-life of $Cln2^{S396A}$ and $Cln2^{S427A}$, we transiently expressed HA-tagged mutant or wild-type genes from the *GAL1* promoter and tracked the abundance of the Cln2 protein for 60 min. These mutations caused a loss of the species of lowest mobility, which is consistent with the loss of sites of in vivo phosphorylation (*12*). The half-life of each mutant protein was increased, from 8 ± 2.5 min for the wild-type Cln2 to 11 ± 3 min for $Cln2^{S396A}$ and 21 ± 2 min for $Cln2^{S427A}$ (Table 1) (*12*). Thus, it appeared that phosphorylation at either of these sites could contribute to the destabilization of Cln2. Alanine substitutions at both Ser^{396} and Ser^{427} ($Cln2^{S396,427A}$) resulted in an increase in the half-life of the Cln2 protein to ~30 min, about half of the stabilization resulting from the elimination of all seven SP and TP sites (Table 1) (*12*). Thus, whereas no single site was sufficient to account for the stabilization associated with the $Cln2^{4T3S}$ mutant, some smaller constellation of sites may be sufficient.

Table 1. Analysis of *CLN2* mutants. The half-life of Cln2 was determined by densitometric analysis. ND, not determined; wt, wild type.

Genotype	Protein steady-state level	Cln2 half-life (min)
Wild type	wt	8
T311A	wt	ND
T381A	wt	ND
T405A	wt	ND
T430A	wt	ND
S396A	>wt	11
S427A	>wt	21
S518A	wt	5
S396, 427A	>>wt	30
4T3S	>>>wt	60
Δ376-514	>>wt	55
Δxs	ND	18
Δxs4T3S	ND	18

Both Ser^{396} and Ser^{427} reside in the COOH-terminus of Cln2, but only Ser^{396} lies within the Cln2 PEST sequence. Mutations outside the PEST sequence are responsible for at least some of the stability of $Cln2^{4T3S}$ (*12*). This is consistent with the finding that elimination of the PEST sequence of Cln2 fails to stabilize Cln2 to the degree observed with the $Cln2^{4T3S}$ mutant (*4*). It is possible that the relevant aspect of PEST sequences is their richness in CDK target sites rather than their PEST amino acids per se.

Our results demonstrate that phosphorylation of Cln2 provides a signal that is necessary for its rapid degradation. However, phosphorylation is of little importance either in terms of its ability to bind and activate the Cdc28 protein kinase or to perform its requisite cell cycle functions. The presence of specific phosphorylated residues may be required for recognition of G_1 cyclins by the protein degradation machinery responsible for their degradation. The elements responsible for that recognition are unknown. Experiments performed in vitro suggest that Cln2 is a substrate for the E2 ubiquitin-conjugating enzyme encoded by the *CDC34* gene (*13, 14*), but inactivation of *CDC34* has been reported to result in only modest stabilization of Cln2 in vivo (*4, 12, 13*). Thus, although it appears likely that Cln2 degradation is mediated by the ubiquitin-proteasome pathway, this has yet to be demonstrated in vivo. In contrast to Cln2, the B-type cyclins require phosphorylation for some aspects of their biological function (*15*) but not for activation of their cognate CDK or for their timely degradation (*16*).

Our results are most consistent with the view that Cdc28 is the primary kinase that phosphorylates Cln2. We have not excluded the possibility that Cln2-Cdc28 complexes might be substrates for another protein kinase. However, a direct role for Cdc28 is supported by the observation that Cln2 participating in a complex with catalytically inactive Cdc28 becomes phosphorylated in cells that also contain functional Cdc28 but not in cells where Cdc28 is inactive (*17*). Cln2 also acts as a substrate of the Cln2-Cdc28 protein kinase in vitro (Fig. 3B) (*18*). Targeting Cln2 for degradation by means of phosphorylation by its cognate CDK provides a mechanism by which activation of the Cdc28 CDK by Cln2 could target that cyclin for degradation, thus rendering it self-limiting. This result, in conjunction with the repression of *CLN2* gene expression that occurs as a consequence of cell cycle progression (*19*), could account for the inactivation of G_1 cyclins as cells leave the G_1 phase.

REFERENCES AND NOTES

1. T. Evans, E. T. Rosenthal, J. Youngbloom, D. Distel, T. Hunt, *Cell* **33**, 389 (1983); K. I. Swenson, K. M. Farrell, J. V. Ruderman, *ibid.* **47**, 861 (1986).
2. C. Wittenberg, K. Sugimoto, S. I. Reed, *ibid.* **62**, 225 (1990).
3. F. R. Cross and C. M. Blake, *Mol. Cell. Biol.* **13**, 3266 (1993); M. Tyers, G. Tokiwa, R. Nash, B. Futcher, *EMBO J.* **11**, 1773 (1992).
4. S. R. Salama, K. B. Hendricks, J. Thorner, *Mol. Cell. Biol.* **14**, 7953 (1994).
5. J. Yaglom *et al.*, *ibid.* **15**, 731 (1995).
6. S. Rogers, R. Wells, M. Rechsteiner, *Science* **234**, 364 (1986).
7. F. Cross, *Mol. Cell. Biol.* **8**, 4675 (1988); R. Nash, G. Tokiwa, S. Anand, K. Erickson, A. B. Futcher, *EMBO J.* **7**, 4335 (1988); J. A. Hadwiger, C. Wittenberg, M. A. de Barros Lopes, H. E. Richardson, S. I. Reed, *Proc. Natl. Acad. Sci. U.S.A.* **86**, 6255 (1989); see also Table 1, *CLN2Δ376-514*, and (*12*).
8. S. Lanker and C. Wittenberg, unpublished results.
9. F. R. Cross and A. H. Tinkelenberg, *Cell* **65**, 875 (1991).
10. M. R. Gerber, A. Farrell, R. J. Deshaies, I. Herskowitz, D. O. Morgan, *Proc. Natl. Acad. Sci. U.S.A.* **92**, 4651 (1995); C. Wittenberg, unpublished results.
11. Abbreviations for the amino acid residues are as follows: A, Ala; C, Cys; D, Asp; E, Glu; F, Phe; G, Gly; H, His; I, Ile; K, Lys; L, Leu; M, Met; N, Asn; P, Pro; Q, Gln; R, Arg; S, Ser; T, Thr; V, Val; W, Trp; and Y, Tyr. Mutations are indicated with this code; for instance, Ser^{396} mutated to Ala is indicated by S396A.
12. S. Lanker, M. H. Valdivieso, C. Wittenberg, unpublished results.
13. R. J. Deshaies, V. Chau, M. Kirschner, *EMBO J.* **14**, 303 (1995).
14. M. Goebl *et al.*, *Science* **241**, 1331 (1988).
15. Li, J., A. N. Meyer, D. J. Donahue, *Mol. Biol. Cell* **6**, 1111 (1995).
16. T. Izumi and J. L. Maller, *Mol. Cell. Biol.* **11**, 3860 (1991).
17. M. H. Valdivieso and C. Wittenberg, unpublished results.
18. R. Littlefield, S. Lanker, C. Wittenberg, unpublished results.
19. A. Amon, M. Tyers, B. Futcher, K. Nasmyth, *Cell* **74**, 993 (1993); D. Stuart and C. Wittenberg, *Genes Dev.* **9**, 2780 (1995).
20. M. Tyers, G. Tokiwa, B. Futcher, *EMBO J.* **12**, 1955 (1993).
21. Final concentrations of phosphatase inhibitors were 10 mM sodium pyrophosphate, 5 mM EDTA, 5 mM EGTA, and 0.1 mM orthovanadate.
22. Tagging of *CLN2* was done by appending to the 3′ end of the *CLN2* open reading frame a DNA fragment encoding three copies of the HA epitope (*20*); D. Stuart, unpublished results]. The various tagged *CLN2* constructs were created by replacing wild-type *CLN2* 3′ ends with the HA-tagged form or by replacing wild-type HA-tagged *CLN2* sequences with fragments containing the mutated site or sites.

23. Logarithmically growing cells were labeled with TRAN-^{35}S label (ICN) [C. Wittenberg and S. I. Reed, *Cell* **54**, 1061 (1988)], and immunoprecipitations were done essentially as described [M. Hochstrasser and A. Varshavsky, *ibid.* **61**, 697 (1990)] with affinity-purified polyclonal antiserum to Cln2.
24. In vivo [^{32}P]orthophosphate labeling of cells was done essentially as described [J. R. Warner, *Methods Enzymol.* **194**, 423 (1991)]. Logarithmically growing cells were starved for phosphate for 6 to 8 hours, concentrated to one-tenth volume, labeled for 20 min with [^{32}P]orthophosphate (1 mCi/ml), diluted with 4 volumes, and incubated for 1 to 2 hours. Sedimented cells were washed once with ice-cold water, and cell lysis and immunoprecipitation were done as described (*20*) with the following modifications. Lysis buffer contained protease inhibitors [0.4 mM phenylmethylsulfonyl fluoride (PMSF) and 1 μg/ml each of leupeptin, pepstatin A, and aprotinin] and a phosphatase inhibitor mixture (*21*) instead of NaF and EDTA. Before immunoprecipitation with monoclonal antibodies to HA, we denatured proteins by adjusting the extract to 1% SDS and 15 mM dithiothreitol and boiling for 2 min. After centrifugation (15 min at 15,000*g*), extracts were diluted with 9 volumes of immunoprecipitation (IP) buffer (50 mM tris-HCl, pH 7.5, 1% Triton X-100, and 250 mM NaCl, plus protease and phosphatase inhibitors as above). Immune complexes on protein A–Sepharose beads were washed three times with IP buffer, incubated for 30 min on ice in IP buffer containing 200 μg/ml of ribonuclease A, washed once with TBS (100 mM tris-HCl, pH 7.5, and 0.9% NaCl), and boiled in 2× sample buffer.
25. I. A. Wilson *et al.*, *Cell* **37**, 767 (1984).
26. Immune complex protein kinase assays were done essentially as described (*13*). Immune complexes were prepared as described (*20*) with the following modifications. Lysis buffer contained protease inhibitors (0.4 mM PMSF and 1 μg/ml each of leupeptin, pepstatin A, and aprotinin) and a phosphatase inhibitor mixture (*21*) instead of NaF and EDTA. For in vitro phosphorylation of Cln2, histone H1 and unlabeled adenosine triphosphate (ATP) were omitted from the assay.
27. W. J. Boyle *et al.*, *Methods Enzymol.* **201**, 110 (1991).
28. C. Wittenberg, S. L. Richardson, S. I. Reed, *J. Cell Biol.* **105**, 1527 (1987).
29. Site-directed mutagenesis was done on subclones of *CLN2* either with the pALTER system (Promega) or with the polymerase chain reaction. Fragments encompassing the mutated site or sites were subcloned into the TA vector (Invitrogen) and verified by sequencing. To create stable integrants, we subcloned mutated *CLN2* alleles containing wild-type 5′ and 3′ untranslated sequences into pUC18 containing a *HIS2* gene and integrated them at the *his2* locus. To create centromeric vectors containing HA-tagged *CLN2* genes under control of the *GAL1* promoter, we replaced 5′ sequences of a 3′ HA-tagged *CLN2* gene (*22*) with a *GAL1-CLN2* fragment excised from YCpG2 (*2*). Fragments containing *GAL1::CLN2(HA)*$_3$ were then cloned into pRS416 [R. S. Sikorski and P. Hieter, *Genetics* **122**, 19 (1989)].
30. Cell size distributions were analyzed with a Coulter Counter Channelyzer. Mean cell size was determined with a Microsoft Excel–based computer program (S. Lanker and C. Wittenberg, unpublished results).
31. G. F. Sprague Jr., *Methods Enzymol.* **194**, 77 (1991).
32. We constructed *CLN2Δxs*^{4T3S} by deleting the Xho I–Sal I DNA fragment of *CLN2*^{4T3S}, thus creating the same deletion within the cyclin box as in Cln2Δxs (*9*).

33. We thank D. Stuart for the initial *CLN2(HA)*$_3$ construct, M. Guaderrama for expert technical assistance, L. Hengst, C. McGowan, P. Russell, and D. Stuart for helpful discussions and critical reading of the manuscript, and S. Reed for his encouragement at a critical juncture. Supported by U.S. Public Health Services grant GM43487 to C.W. S.L. acknowledges Swiss National Science Foundation and Human Frontier Science Program fellowships. M.H.V. was supported by the Fundación Ramón Areces, Madrid, Spain.

24 October 1995; accepted 1 February 1996

Control of the Gene *optomotor-blind* in *Drosophila* Wing Development by *decapentaplegic* and *wingless*

Stefan Grimm and Gert O. Pflugfelder*

Diffusible factors of several protein families control appendage outgrowth and patterning in both insects and vertebrates. In *Drosophila* wing development, the gene *decapentaplegic* (*dpp*) is expressed along the anteroposterior compartment boundary. Early *wingless* (*wg*) expression is involved in setting up the dorsoventral boundary. Interaction between *dpp*- and *wg*-expressing cells promotes appendage outgrowth. Here, it is shown that *optomotor-blind* (*omb*) expression is required for distal wing development and is controlled by both *dpp* and *wg*. Ectopic *omb* expression can lead to the growth of additional wings. Thus, *omb* is essential for wing development and is controlled by two signaling pathways.

Appendage development in both insects (*1–10*) and vertebrates (*11*) is controlled by conserved diffusible proteins. In *Drosophila*, the wing primordium is divided into compartments by the stable inheritance of selector gene activity (*12*). Appendage development requires the interaction between cells across compartment boundaries. In the wing disc, diffusing HEDGEHOG (HH) protein, synthesized in the posterior compartment under the control of one or more posterior selector genes, directs *dpp* expression in the anterior compartment along the anteroposterior (a-p) boundary (*5*, *12*). DPP is required for patterning on both sides of the a-p boundary (*10*). Similarly, the dorsal selector gene *apterous* (*ap*) promotes the synthesis of the diffusible protein FRINGE (*13*). Early *wg* expression is required for establishing the dorsoventral (d-v) boundary (*2*, *3*). Interaction between *wg*- and *dpp*-expressing cells promotes the development of the proximodistal (p-d) axis (*4–8*). The presumptive transcription factor OMB plays a critical role in the development of the optic lobes, but it is also essential for the development of the distal wing disc (*14*). We investigated the function of *omb* in wing development and analyzed its relation to *dpp* and *wg*.

Lethal *omb* mutants that survived to the pharate adult stage had severely reduced wings (Fig. 1B). The hypomorphic allele *bifid* [*omb*^{bi}, (*14*)] caused the proximal fusion of all longitudinal veins and led to variable defects at the distal tip of the wing (Fig. 1C). Defects in both regions of the wing blade were enhanced by *omb* null alleles (Fig. 1D) and, dominantly, by mutations in genes required for d-v and a-p patterning

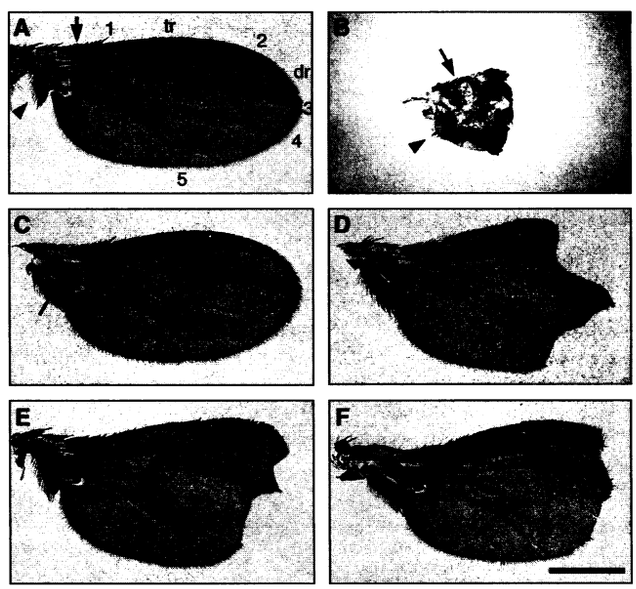

Fig. 1. Wing phenotypes of *omb* alleles and their genetic interactions with d-v and a-p wing patterning genes. (**A**) Pattern elements in the wild-type wing. The longitudinal veins 1 through 5 are numbered where they intersect the wing margin. Triple (tr) and double row (dr) are specializations of the wing margin. The arrow and arrowhead point to anterior (costa) and posterior (alula) elements, respectively. (**B**) Wing from a *l(1)omb*^{3198} (*14*) pharate adult. The proximal elements costa (arrow) and alula (arrowhead) are marked. (**C**) Wing of hypomorphic *omb*^{bi} allele (*14*). All longitudinal veins are fused at the base of the wing (arrow). Distal defects (arrowhead) are variable and temperature-dependent. (**D**) The bifid phenotype is enhanced in combination with all extant lethal *omb* alleles [here, transheterozygote *omb*^{bi}/*l(1)omb*^{3198}]. (**E** and **F**) Dominant enhancement of the omb^{bi} phenotype in *omb*^{bi}/*Y*; *ap*^{56f}/+ (E) and *omb*^{bi}/*Y*; *dpp*^{d8}/+ (F) individuals. The scale bar in (F) (which applies to all panels) represents 0.5 mm.